

Information Scrambling in Bosonic Gaussian Dynamics

Ali Mollabashi and Saleh Rahimi-Keshari

School of Physics, Institute for Research in Fundamental Sciences (IPM), 19538-33511, Tehran, Iran

We show that randomness in quadratic bosonic Hamiltonians results in certain information scrambling diagnostics, mirroring those in chaotic systems. Specifically, for initial Gaussian states, we observe the disappearance of the memory effect in the entanglement dynamics of disjoint blocks and the negative values of tripartite mutual information. We also find that the spectral form factor for these integrable systems exhibits a ramp. However, in contrast to chaotic systems, the ramp is nonlinear, and the out-of-time-ordered correlators display power-law growth for certain operators and Gaussian dynamics. These findings indicate that information scrambling driven by randomness is distinct from quantum chaos. Moreover, our results provide insight into the dynamics of Gaussian states in continuous-variable systems, which are useful and available resources for quantum information processing.

Introduction. Originating from the black-hole information paradox, scrambling of quantum information has become a central feature differentiating between integrable systems and chaotic systems [1–3]. Several diagnostics have been proposed to identify information scrambling such as the spectral form factor (SFF) [4–6], operator entanglement [7–11], entanglement spread [12–17], out-of-time-ordered correlators (OTOC) [3, 18–21] and tripartite mutual information (TMI) [21–23]. However, it has recently been shown that observing an information scrambling diagnostic does not necessarily imply quantum chaos in the system. Specifically, non-chaotic/integrable systems have been identified that exhibit the exponential growth of OTOC [24–26] and operator entanglement [27].

These recent observations raise the question of how quantum information scrambling, distinct from quantum chaos, should be characterized in quantum systems. In particular, identifying the features that drive information scrambling can provide insight into the dynamics of complex quantum systems.

In this paper, we investigate quantum information scrambling in multimode bosonic systems with quadratic Hamiltonians. These systems are integrable however, with a sufficient amount of randomness in the Hamiltonian, admit single-particle chaos [28, 29], i.e. the single-particle sector of the Hilbert space is characterized by random-matrix-like level statistics. We examine different amounts of randomness, ranging from the local translational invariant to the completely random non-local models [30]. For initial Gaussian states and with even a small amount of randomness, preserving the locality

but removing translational invariance in the dynamics, we observe the vanishing of the memory effect during the spread of entanglement of disjoint intervals and the negative values of TMI. We also observe the same features for the tensor product of single-mode squeezed-vacuum states subjected to random Gaussian dynamics generated by passive linear-optical networks. Remarkably, in this case, these features persist even if added noise to the initial states makes them classical and destroys entanglement. These results imply scrambling of information in these systems, similar to what has been predicted for holographic states [13, 31].

We also consider the SFF and OTOC as other information scrambling diagnostics for these systems. We observe that the SFF exhibits a dip followed by a ramp, attributed to the single-particle sector of the Hamiltonian. However, we find non-linear ramps, deviating from the expected behavior in chaotic systems. Additionally, we show that the OTOC displays a power law growth, distinct from the exponential growth seen in chaotic systems. Consequently, these diagnostic tools remain unaffected by the randomness added to the dynamics of the system.

Our study not only sheds light on new aspects of information scrambling but also offers new insights into the dynamics of continuous-variable systems. Gaussian states of these systems are particularly intriguing because of their experimental accessibility. Specifically, quadratic Hamiltonians for bosonic systems lead to Gaussian dynamics, which can be efficiently simulated using linear optical circuits [32]. These circuits are readily accessible and have been used in Gaussian boson sampling experi-

ments [33–36]. Therefore, our results can be experimentally verified and applied to investigate the presence of randomness in the dynamics of such systems.

This paper is structured as follows. We first explain the setup, including Gaussian states and quadratic Hamiltonian models that we use. Then, we report our results on the dynamics of entanglement, TMI, SFF, and OTOC in the presence of randomness in the Hamiltonian.

Setup. We consider N -mode bosonic systems described by the vector of quadrature operators $r = (q_1, \dots, q_N, p_1, \dots, p_N)^\top$, satisfying the canonical commutation relations $[q_j, p_k] = i\delta_{jk}$ ($\hbar = 1$). Quantum states are described by density operators ρ ($\rho \succeq 0$ and $\text{tr}(\rho) = 1$), and those that can be represented by a Gaussian Wigner function can represent are known as Gaussian states [32, 37]. These states can be uniquely characterized using the first-order moment vector $\langle r \rangle = \text{tr}(\rho r)$ and the covariance matrix with the matrix elements given by $\sigma_{jk} = \langle r_j r_k + r_k r_j \rangle - 2\langle r_j \rangle \langle r_k \rangle$. The covariance matrix is symmetric and positive and satisfies the uncertainty relation $\sigma + i\mathbf{J} \geq 0$, where \mathbf{J} is the symplectic form whose matrix elements are given by $\mathbf{J}_{jk} = i[r_k, r_j]$. Reduced states of a Gaussian state with the covariance matrix σ are Gaussian states whose covariance matrices are submatrices of σ . We consider states with $\langle r \rangle = 0$, as this condition can always be satisfied by using local unitary displacement operations. If a covariance matrix satisfies $\sigma - \mathbb{1}_{2N} \geq 0$, where $\mathbb{1}_{2N}$ is the $2N \times 2N$ identity matrix, the corresponding state is *classical* and can be expressed as a statistical mixture of product coherent states. A special example is the product thermal state of N -mode system whose $\langle r \rangle = 0$ and $\sigma_{\text{th}} = \text{diag}(\nu_1, \dots, \nu_N, \nu_1, \dots, \nu_N)$, where $\nu_k \geq 1$ with $\nu_k = 1$ corresponding to the vacuum state in the k th mode.

Unitary transformations that preserve the Gaussianity of quantum states are known as Gaussian unitaries. Up to local displacement operations, Gaussian unitaries are associated with quadratic Hamiltonians of this form

$$H = \frac{1}{2} r^\top \mathbf{M} r \quad (1)$$

with matrix \mathbf{M} being real, symmetric, and positive definite [38]. Such Gaussian unitary can be described by $e^{iHt} r e^{-iHt} = \mathbf{S} r$, where $\mathbf{S} = e^{\mathbf{J}\mathbf{M}t}$ is a symplectic matrix, satisfying $\mathbf{S}\mathbf{J}\mathbf{S}^\top = \mathbf{J}$. Using this, one can see that the evolution of Gaussian states under Gaussian unitaries, $\rho_t = e^{-iHt} \rho e^{iHt}$, can be described in terms of symplectic transformations on the covariance matrices,

$\sigma_t = \mathbf{S} \sigma \mathbf{S}^\top$. Gaussian unitaries with orthogonal symplectic matrices, preserve the mean energy of the system and are known as passive transformations. In quantum optics, these transformations can be realized using linear-optical networks.

According to the Euler decomposition, any Gaussian unitary can be expressed as $U_p \otimes_{j=1}^N U_{\text{sq}, \lambda_j} \tilde{U}_p$, where U_p and \tilde{U}_p are passive multimode unitaries, and U_{sq, λ_j} are single-mode squeezing unitaries, described by $U_{\text{sq}, \lambda_j}^\dagger(q_j, p_j) U_{\text{sq}, \lambda_j} = (q_j e^{-\lambda_j}, p_j e^{\lambda_j})$. Williamson's theorem states that a Gaussian unitary can transform any Gaussian state into a thermal state. This implies that covariance matrices can be diagonalized using symplectic transformations, $\sigma = \mathbf{S} \text{diag}(\nu_1, \dots, \nu_N, \nu_1, \dots, \nu_N) \mathbf{S}^\top$, where ν_k are known as the symplectic eigenvalues. Considering this theorem and noting that passive unitaries do not change the vacuum state, we can see that any pure Gaussian state can be constructed by applying single-mode squeezing unitaries on the vacuum state followed by a multimode passive Gaussian unitary. Note also that one can see that the von Neumann entropy of Gaussian states can be expressed in terms of the symplectic eigenvalues $\sum_k \left[\frac{\nu_k+1}{2} \ln\left(\frac{\nu_k+1}{2}\right) - \frac{\nu_k-1}{2} \ln\left(\frac{\nu_k-1}{2}\right) \right]$.

Gaussian states can also be viewed as a thermal state of a quadratic Hamiltonian $\rho = e^{-\beta H} / \text{tr}(e^{-\beta H})$ [37]. In this view, Williamson's theorem implies that the Hamiltonian can be uncoupled by a Gaussian unitary $U^\dagger H U = \sum_{j=1}^N \omega_j (q_j^2 + p_j^2)$, where ω_j are the frequencies of the uncoupled modes, known as normal modes. Here, the Gaussian unitary U corresponds to the symplectic transformation that diagonalizes the Hamiltonian matrix $\mathbf{S}^\top \mathbf{M} \mathbf{S} = \text{diag}(\omega_1, \dots, \omega_N, \omega_1, \dots, \omega_N)$. Using this Gaussian unitary, we can obtain the Hamiltonian's ground state from the uncoupled Hamiltonian's vacuum state.

Local Hamiltonians. Let us first consider N harmonic oscillators on a one-dimensional chain with the nearest-neighbor couplings and periodic boundary conditions. The general form of the Hamiltonian reads

$$H_{\mu, \kappa} = \frac{1}{2} \sum_{n=1}^N \left[\frac{p_n^2}{\mu} + \mu m^2 q_n^2 + \kappa (q_{n+1} - q_n)^2 \right]. \quad (2)$$

By using local squeezing operations $U_{\text{sq}, \lambda}$ on each harmonic oscillator with $e^{2\lambda} = \sqrt{\mu\kappa}$ and defining $\epsilon = \sqrt{\mu/\kappa}$, this Hamiltonian can be transformed into

$$H_\epsilon = \frac{1}{2} \sum_{n=1}^N \left[\frac{p_n^2}{\epsilon} + \epsilon m^2 q_n^2 + \frac{1}{\epsilon} (q_{n+1} - q_n)^2 \right]. \quad (3)$$

This Hamiltonian known as the harmonic lattice model describes a Klein-Gordon (KG) free massive scalar field in two-dimensional spacetime, regularized on a lattice with the spacing ϵ and mass m . To recover the continuum limit, we have to take the limit of $\epsilon \rightarrow 0$. We, however, consider a *non-vanishing* lattice spacing, corresponding to a UV cut-off in the field theory description. For convenience, hereafter, we set $\epsilon = 1$ and $H_{\text{KG}} = H_1$.

The Hamiltonian matrix in (3) includes an $N \times N$ circulant matrix $\text{circ}(m^2 + 2, -1, 0, \dots, 0, -1)$, whose eigenvalues are $m^2 + (2\sin(\pi(j-1)/N))^2$ for $j = 1, \dots, N$. By ordering the eigenvalues $\omega_1^2 \leq \omega_2^2 \leq \dots \leq \omega_N^2$, an orthogonal matrix \mathbf{V} that diagonalizes this matrix can be found as follows. Defining row vectors $F_j = \frac{1}{\sqrt{N}}(1, \nu^{(N+1-j)}, \dots, \nu^{(N-1)(N+1-j)})$ with $\nu = \exp(2\pi i/N)$, the first row of \mathbf{V} is given by $V_1 = F_1$, other rows are given by $V_{2k} = (F_{k+1} + F_{N-k+1})/\sqrt{2}$ and $V_{2k+1} = i(F_{k+1} - F_{N-k+1})/\sqrt{2}$ for $1 \leq k < N/2$, and if N is even the last row becomes $V_N = F_{\frac{N}{2}+1}$. Using this, the Hamiltonian matrix in (3) can be diagonalized by the symplectic matrix $\mathbf{S}_p = \mathbf{V} \oplus \mathbf{V}$, corresponding to a passive Gaussian unitary U_p . Applying this unitary on the Hamiltonian gives $U_p^\dagger H U_p = \sum_{j=1}^N (\omega_j^2 q_j^2 + p_j^2)$. Therefore, by using additional local squeezing transformations $\otimes_{j=1}^N U_{\text{sq}, \lambda_j}$ with squeezing parameters $\lambda_j = \frac{1}{2} \log \omega_j$, we obtain the Hamiltonian of uncoupled harmonic oscillators $\sum_{j=1}^N \omega_j^2 (q_j^2 + p_j^2)$.

The ground state of Hamiltonian (3) is a Gaussian state of N mode, which can be prepared in quantum optical settings by applying local squeezing operations $\otimes_{j=1}^N U_{\text{sq}, \lambda_j}$ on the vacuum state of each mode, followed by an N -mode passive linear optical transformation described by orthogonal matrix \mathbf{V} . This analogy provides an operational cost of reaching the conformal field theory regime. Note that to reach this scale-invariant regime, we need to take the limit of $m \rightarrow 0$. However, since $\omega_1 = m$, taking this limit implies infinite squeezing $\lambda_1 \rightarrow -\infty$, meaning that preparing the ground state in the scale-invariant regime requires infinite energy.

Random Gaussian Unitary Dynamics. We now describe our models of random Gaussian dynamics to investigate information scrambling. The first model (I) is a disordered version of the local Hamiltonian (3)

$$H_{\text{DKG}} = \frac{1}{2} \sum_{n=1}^N \left[\frac{p_n^2}{\epsilon} + \epsilon m^2 q_n^2 + \frac{J_n}{\epsilon} (q_{n+1} - q_n)^2 \right]. \quad (4)$$

where J_n are random real numbers. We denote this local Hamiltonian with random interactions by the disordered Klein-Gordon (DKG) Hamiltonian.

We also consider models in terms of passive linear-optical circuits to generate random Gaussian dynamics. The initial state is the tensor product of N single-mode squeezed vacuum states, $\otimes_{j=1}^N U_{\text{sq}, \lambda_j} |0, \dots, 0\rangle$. In the first circuit model (IIa), a passive N -mode linear-optical network acts on the initial state in one step. The unitary operator U_p linearly transforms the creation operators, $U_p^\dagger a_j^\dagger U_p = \sum_n U_{jn} a_n^\dagger$, where U_{jn} are the elements of an $N \times N$ unitary transfer matrix \mathbf{U} , which describes the network. We choose matrix \mathbf{U} from a Haar measure to induce randomness, and the corresponding symplectic matrix is given by $\mathbf{S}_p = \begin{pmatrix} \text{Re}(\mathbf{U}) & \text{Im}(\mathbf{U}) \\ -\text{Im}(\mathbf{U}) & \text{Re}(\mathbf{U}) \end{pmatrix}$. In the second circuit model (IIb), two layers of beam splitters described by $\otimes_{j=1} U_{\text{BS}, 2j} \otimes_{j=1} U_{\text{BS}, 2j-1}$ act on the N -mode state in each time step. We assume periodic boundary conditions, and the beam splitter operator $U_{\text{BS}, j}$, which is the 2-mode version of passive linear-optical networks, acts on j th and $(j+1)$ th modes. We also choose the beam-splitter transfer matrix \mathbf{U}_{BS} from a Haar measure to generate random dynamics.

In addition to the above random models, we consider the completely random model (IIIa), where the Hamiltonian matrix \mathbf{M} in Eq. (1) is chosen from the Gaussian symplectic ensemble (GSE). We also consider another model (IIIb) with block diagonal Hamiltonian matrix $\mathbf{M} = \text{diag}((\mathbf{M}_q + \mathbf{M}_q^\dagger)/2, \mathbf{1}_N)$, where \mathbf{M}_q is chosen from either the Gaussian orthogonal ensemble (GOE) or the Gaussian unitary ensemble (GUE).

Memory Effect During Entanglement Dynamics. The pattern of entanglement dynamics of disjoint blocks is a distinct measure of information scrambling. Here we denote these blocks by A_1 and A_2 separated by d with $d > \ell_{A_1}, \ell_{A_2}$. Characterizing this measure originates in a holographic viewpoint wherein maximally chaotic systems are realized by holographic conformal field theories (CFTs) [39]. The joint entropy $S_{A_1 \cup A_2}(t)$ in integrable systems (e.g. free CFTs) shows a long-term *memory effect*, namely a dip-ramp occurring after saturation, that is absent in chaotic systems (e.g. holographic CFTs) [13]. Such a behavior has been realized in a wide spectrum of systems [13, 15–17, 40–44]. This effect indicates that initially uncorrelated A_1 and A_2 become correlated during the period of dip-ramp formation [45]. The propagation

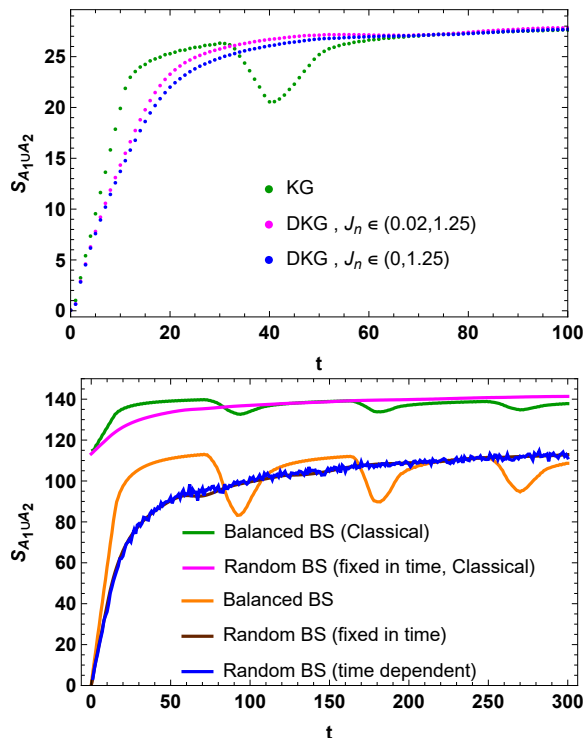


FIG. 1. The disappearance of the memory effect, the dip in the time evolution of the joint entropy $S_{A_1 \cup A_2}$, as an information scrambling diagnostic in the presence of randomness in the dynamics. Upper panel: $S_{A_1 \cup A_2}$ in KG versus DKG models. The ground state of H_{KG} with $m = 2$, denoted by $|\psi_{\text{KG},0}\rangle$ is evolved by unitary operators associated with H_{KG} with $m = 10^{-7}$ (such a process is sometimes called a mass quench) and H_{DKG} with same value of m . We set the number of modes in the disjoint intervals $N_{A_1} = N_{A_2} = 20$, the separation between them $d = 60$, and the system size $N = 500$. Lower panel: $S_{A_1 \cup A_2}$ in the passive circuit model (IIb). The initial state is the tensor product of single-mode squeezed vacuum states with $\lambda_i = 2$. We set $N_{A_1} = N_{A_2} = 40$ and $d = 200$. We consider two scenarios: the beam splitter (BS) transfer matrix \mathbf{U}_{BS} is chosen randomly at every single time step, and \mathbf{U}_{BS} is fixed during the evolution. For a balanced BS, we observe memory effects, where the second and third dips in the orange curve correspond to entanglement revivals. We observe a similar effect if we add vacuum noise to the squeezed-vacuum states to make the initial state classical and destroy entanglement in the states. All random results are averaged over 300 samples.

of free-streaming quasi-particles can describe this effect: those pairs of quasiparticles originating from the gap between A_1 and A_2 and simultaneously present in A_1 and A_2 are responsible for the dip-ramp [46–48].

We consider the ground state of H_{KG} with $m \neq 0$, de-

noted by $|\psi_{\text{KG},0}\rangle$, as the initial state. The upper panel of Fig. 1 presents our simulation results for the joint entropy when the unitary evolution of $|\psi_{\text{KG},0}\rangle$ is induced by H_{KG} with $m \rightarrow 0$ (corresponding to free bosonic CFT with unit central charge), showing an apparent memory effect, versus H_{DKG} with the same m , showing no memory effect. We find similar behavior with the passive circuit model (IIb) presented in the lower panel. Note that in an integrable periodic system, the correlation between A_1 and A_2 revives periodically, known as entanglement revivals [49–51]. This effect can be observed in the lower panel of Fig. 1 for a balanced beam splitter with $\mathbf{U}_{\text{BS}} = (\mathbb{1}_2 + i\mathbf{X})/\sqrt{2}$, where \mathbf{X} is the X -Pauli matrix, while the memory effect disappears for the case of random beam splitters as another sign of scrambling in these systems [52, 53]. Interestingly, we observe the same features, as shown in the lower panel of Fig. 1, even if one unit of vacuum noise is added to the initial squeezed-vacuum states of the model (IIb). In this case, the initial state is the tensor product of states with the covariance matrix $\text{diag}(e^{-2\lambda} + 1, e^{2\lambda} + 1)$, which are classical, and since passive networks transform product coherent states into product coherent states [54], no entanglement is generated through the network. Note that we can still see shallow dips in the case of balanced beam splitters even though there is no entanglement in the system. This effect may be associated with the wave interference of classical states through the dynamics.

Tripartite Mutual Information. Tripartite mutual information is defined in terms of mutual information $I_2(A_1 : A_2) = S_{A_1} + S_{A_2} - S_{A_1 \cup A_2}$ as

$$I_3 = I_2(A_1 : A_2) + I_2(A_2 : A_3) - I_2(A_2 : A_1 \cup A_3).$$

The sign of I_3 is not definite in general [55–58] though in holographic theories $I_3 \leq 0$ [31]. Negative TMI is considered a sign of information scrambling in dynamical systems [21]. Such a behavior has been realized in a range of many body systems [22, 23, 59–62].

We show that the sign of TMI for Gaussian states evolved by a unitary with some randomness takes a non-positive value. In the upper panel of Fig. 2, we show this for the initial state $|\psi_{\text{KG},0}\rangle$ evolved by unitary operators associated with H_{DKG} with $m = 10^{-7}$. In the lower panel, we show the same effect for generic subregion configurations in our random model (IIa), where the tensor product of single-mode squeezed vacuum states is evolved by a Haar random passive linear-optical network.

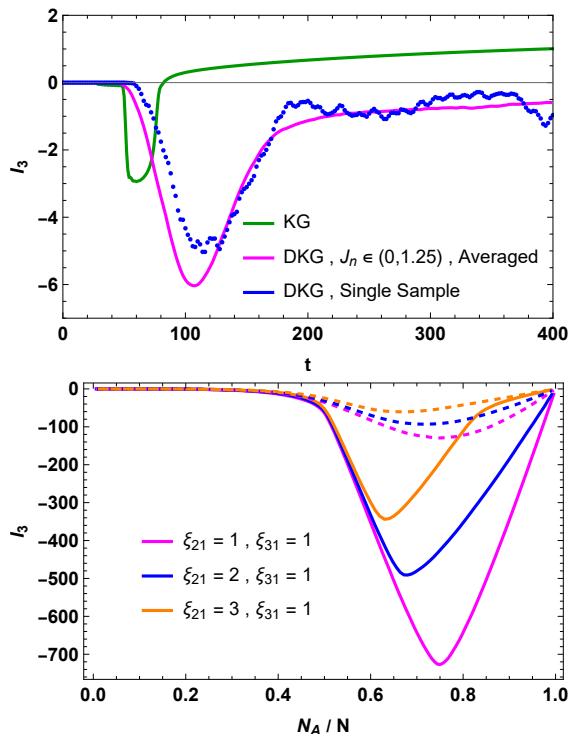


FIG. 2. Negative TMI in the presence of randomness in the dynamics as an indication of information scrambling. Upper panel: I_3 in KG versus DKG through a quenching process similar to Fig. 1. DKG results are averaged over 100 samples. We consider adjacent intervals $N_{A_1} = N_{A_2} = N_{A_3} = 50$ and $N = 1000$. Lower panel: I_3 for random model (IIa), where the tensor product of squeezed-vacuum states ($\lambda_i = 5$) is evolved by a one-step N -mode passive network described by a Haar random unitary. We set $N = 500$ and $\xi_{ij} \equiv \frac{N_{A_i}}{N_{A_j}}$. The dashed curves correspond to the same parameters as the solid curves but one unit of vacuum noise is added to the initial squeezed-vacuum states to make them classical. In this case, no entanglement is generated in the network.

As shown in Fig. 2, TMI can still be negative even if the initial squeezed states are replaced by the classical states described above, and hence there is no entanglement in the final state. We have verified this behavior in various setups with different amounts of randomness.

Spectral Form Factor. Compared to the nearest neighbor level statistics, SFF captures many particle level statistics. In our case in terms of the normal modes, SFF is defined for the k th mode in terms of the non-normalized single-mode partition function $Z_k(\beta) =$

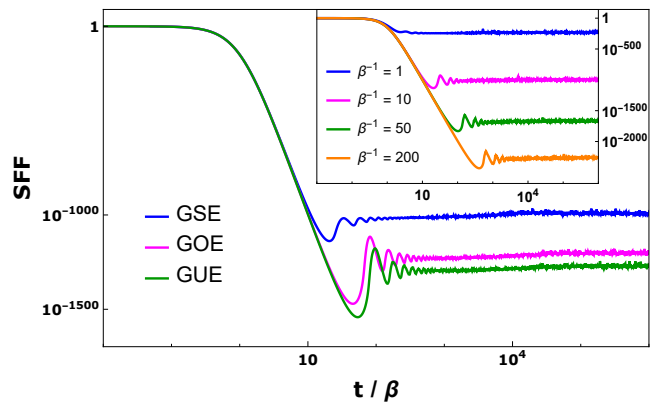


FIG. 3. We observe a dip followed by a non-linear ramp in SFF. We use $\beta^{-1} = 500$ for the random model (IIIa) with $M \in \text{GSE}$, and $\beta^{-1} = 1000$ for the random model (IIIb) with $M_q \in \text{GOE}, \text{GUE}$. The inset corresponds to the DKG Hamiltonian with $J_n \in (0.5, 1.5)$. The system size is $N = 500$ averaged over 100 samples.

$\sum_{n_k} e^{-\beta \omega_k n_k}$ as

$$g_k(\beta, t) = \frac{|Z_k(\beta + it)|^2}{|Z_k(\beta)|^2} = \frac{\cosh(\beta \omega_k) - 1}{\cosh(\beta \omega_k) - \cos(\omega_k t)},$$

and SFF for the whole system is given by $g(\beta, t) = \Pi_k g_k(\beta, t)$. We numerically average $g(\beta, t)$ over thermal states, sometimes called as the quenched quantity.

While ergodic chaotic systems are known to exhibit a linear ramp at intermediate times, nonergodic integrable systems are not expected to show a ramp. Figure 3 shows our numerical results where we find a dip followed by a non-linear ramp for random models (IIIa) with $M \in \text{GSE}$ and (IIIb) with $M_q \in \text{GOE}, \text{GUE}$. In all the cases, we see that the elevation of the non-linear ramp is proportional to the amount of randomness in the model. Note that an exponential ramp has been reported for SYK₂ in [28, 29].

Out of Time-Ordered Correlators. OTOC has been defined by quantizing the classical observation that the sensitivity to the initial conditions can be quantified by the Poisson bracket $\{q(t), p\}$ [3, 18, 63]. Although the old paradigm expresses the exponential growth of OTOC and quantum chaos as reciprocal notions [3], in the current understanding an unstable saddle point in integrable systems can lead to the exponential growth of OTOC [25]. A natural question is how OTOC behaves in integrable systems in the presence of randomness.

Here we consider OTOC in terms of the canonical op-

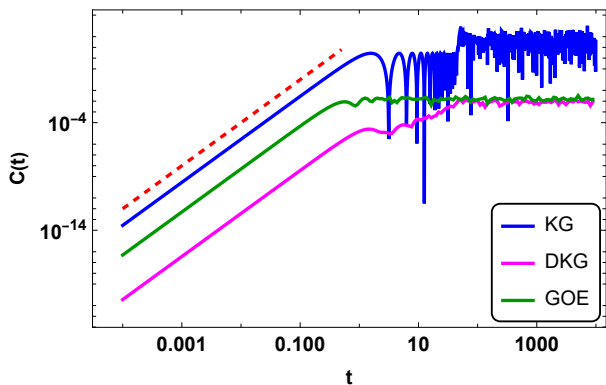


FIG. 4. OTOC for $q_j(t)$ and p_k in the ground state of the KG, DKG and model (IIIb) Hamiltonians, showing a power law growth. We set $j = 1$, $k = N/2$, and $N = 100$. The DKG and GOE results are averaged over 100 samples. The dashed red line $\propto t^4$.

erators

$$C_{\beta,jk}(t) = -\text{tr} \left(\frac{e^{-\beta H}}{\text{tr}(e^{-\beta H})} [q_j(t), p_k]^2 \right) \quad (5)$$

where $q_j(t) = e^{itH} q_j e^{-itH}$ and j, k stands for the mode index. For the cases of KG, DKG, random model (IIIb) as well as any Hamiltonian matrix that can be diagonalized with a symplectic transformation of the form $\mathbf{S} = \mathbf{S}_q \oplus \mathbf{S}_p$, we find (see Appendix A)

$$C_{\infty,jk}(t) = (\mathbf{S}_q \text{diag}(\cos(\omega_1 t), \dots, \cos(\omega_N t)) \mathbf{S}_p^T)_{jk}^2, \quad (6)$$

where $\beta \rightarrow \infty$ implies zero temperature and the OTOC is with respect to the ground state of the Hamiltonian. In this case, using $\mathbf{S}_q \mathbf{S}_p^T = \mathbb{1}_N$, one can easily verify that $C_{\infty,jk}(t \ll 1) \sim t^4$ for $k \neq j$ and $C_{\infty,jk}(t \ll 1) \sim t^2$ for $k = j$. Our detailed analytic analysis and the numerical simulation shown in Fig. 4 perfectly agree with this result.

In Appendix B, we analyze a generic form of OTOC for passive Hamiltonians. At zero temperature, this quantity depends on a single time-dependent parameter, whose saturation time decreases with the number of modes, as $t_* \sim 1/\log N$. This feature results in shortening the power law growth in large systems followed by a plateau.

Discussions. We have shown that randomness in integrable bosonic systems leads to information scrambling, characterized by the disappearance of the memory effect in the spread of entanglement, negative values of TMI, and the presence of a ramp in SFF. These results identify

information scrambling associated with randomness as a distinct feature from quantum chaos.

An interesting feature of our results is that this form of information scrambling can be observed in the Gaussian states of continuous-variable systems that are useful resources in quantum information processing. We note that Gaussian states and Gaussian dynamics can be efficiently described in terms of the Wigner function. As we have shown in Appendix C, similar results can be obtained in terms of the Rényi-2 entropy, which is linked to the continuous Shannon entropy of classical random variables generated according to the Wigner function [64]. This implies that the information scrambling diagnostics can be analogously observed in classical systems.

Our study should not be mixed with what has been addressed as *weak scrambling* in nonrandom local integrable systems [17]. There is no global scrambling effect in such systems; rather, it is a local effect in the sense that recovering the initial data of a subregion would require measurements in a larger subregion. This effect is enhanced in Lifshitz models due to non-linear dispersion resulting in infinitely prolonged saturation time for the entanglement of finite subregions [65].

Among several open questions about random integrable models, an interesting one would be the description of the dynamical behaviors discussed here regarding ballistically propagating quasiparticles. Another interesting direction would be investigating possible semiclassical descriptions for such quadratic systems.

Acknowledgments: We thank Reza Mohammadi Mozaffar, Salman Beigi and Pratik Nandy for useful discussions. AM would like to acknowledge support from ICTP through the Associates Programme (2023-2028) and for hospitality during stages of this work.

-
- [1] P. Hayden and J. Preskill, Black holes as mirrors: Quantum information in random subsystems, *JHEP* **09**, 120, [arXiv:0708.4025 \[hep-th\]](#).
 - [2] Y. Sekino and L. Susskind, Fast Scramblers, *JHEP* **10**, 065, [arXiv:0808.2096 \[hep-th\]](#).
 - [3] S. H. Shenker and D. Stanford, Black holes and the butterfly effect, *JHEP* **03**, 067, [arXiv:1306.0622 \[hep-th\]](#).
 - [4] E. Brézin and S. Hikami, Spectral form factor in a random matrix theory, *Phys. Rev. E* **55**, 4067 (1997).
 - [5] F. Haake, *Quantum Signatures of Chaos*, Springer Series in Synergetics (Springer, Berlin, 2010).

- [6] J. S. Cotler, G. Gur-Ari, M. Hanada, J. Polchinski, P. Saad, S. H. Shenker, D. Stanford, A. Streicher, and M. Tezuka, Black Holes and Random Matrices, *JHEP* **05**, 118, [Erratum: *JHEP* 09, 002 (2018)], [arXiv:1611.04650 \[hep-th\]](#).
- [7] P. Zanardi, Entanglement of quantum evolutions, *Phys. Rev. A* **63**, 040304 (2001), [arXiv:quant-ph/0010074](#).
- [8] V. Alba, J. Dubail, and M. Medenjak, Operator Entanglement in Interacting Integrable Quantum Systems: The Case of the Rule 54 Chain, *Phys. Rev. Lett.* **122**, 250603 (2019), [arXiv:1901.04521 \[cond-mat.stat-mech\]](#).
- [9] B. Bertini, P. Kos, and T. Prosen, Operator Entanglement in Local Quantum Circuits I: Chaotic Dual-Unitary Circuits, *SciPost Phys.* **8**, 067 (2020), [arXiv:1909.07407 \[cond-mat.stat-mech\]](#).
- [10] L. Nie, M. Nozaki, S. Ryu, and M. T. Tan, Signature of quantum chaos in operator entanglement in 2d CFTs, *J. Stat. Mech.* **1909**, 093107 (2019), [arXiv:1812.00013 \[hep-th\]](#).
- [11] G. Styliaris, N. Anand, and P. Zanardi, Information Scrambling over Bipartitions: Equilibration, Entropy Production, and Typicality, *Phys. Rev. Lett.* **126**, 030601 (2021), [arXiv:2007.08570 \[quant-ph\]](#).
- [12] N. Lashkari, D. Stanford, M. Hastings, T. Osborne, and P. Hayden, Towards the Fast Scrambling Conjecture, *JHEP* **04**, 022, [arXiv:1111.6580 \[hep-th\]](#).
- [13] C. T. Asplund, A. Bernamonti, F. Galli, and T. Hartman, Entanglement Scrambling in 2d Conformal Field Theory, *JHEP* **09**, 110, [arXiv:1506.03772 \[hep-th\]](#).
- [14] Z.-W. Liu, S. Lloyd, E. Y. Zhu, and H. Zhu, Entanglement, quantum randomness, and complexity beyond scrambling, *JHEP* **07**, 041, [arXiv:1703.08104 \[quant-ph\]](#).
- [15] A. Nahum, J. Ruhman, S. Vijay, and J. Haah, Quantum entanglement growth under random unitary dynamics, *Phys. Rev. X* **7**, 031016 (2017).
- [16] B. Bertini, P. Kos, and T. c. v. Prosen, Entanglement spreading in a minimal model of maximal many-body quantum chaos, *Phys. Rev. X* **9**, 021033 (2019).
- [17] V. Alba and P. Calabrese, Quantum information scrambling after a quantum quench, *Phys. Rev. B* **100**, 115150 (2019), [arXiv:1903.09176 \[cond-mat.stat-mech\]](#).
- [18] A. Larkin and Y. Ovchinnikov, Quasiclassical method in the theory of superconductivity, *JETP* **28** (1969).
- [19] J. Maldacena, S. H. Shenker, and D. Stanford, A bound on chaos, *JHEP* **08**, 106, [arXiv:1503.01409 \[hep-th\]](#).
- [20] D. A. Roberts and D. Stanford, Two-dimensional conformal field theory and the butterfly effect, *Phys. Rev. Lett.* **115**, 131603 (2015), [arXiv:1412.5123 \[hep-th\]](#).
- [21] P. Hosur, X.-L. Qi, D. A. Roberts, and B. Yoshida, Chaos in quantum channels, *JHEP* **02**, 004, [arXiv:1511.04021 \[hep-th\]](#).
- [22] E. Iyoda and T. Sagawa, Scrambling of Quantum Information in Quantum Many-Body Systems, *Phys. Rev. A* **97**, 042330 (2018), [arXiv:1704.04850 \[cond-mat.stat-mech\]](#).
- [23] S. Pappalardi, A. Russomanno, B. Žunkovič, F. Iemini, A. Silva, and R. Fazio, Scrambling and entanglement spreading in long-range spin chains, *Phys. Rev. B* **98**, 134303 (2018), [arXiv:1806.00022 \[quant-ph\]](#).
- [24] S. Pilatowsky-Cameo, J. Chávez-Carlos, M. A. Bastarrachea-Magnani, P. Stránský, S. Lerma-Hernández, L. F. Santos, and J. G. Hirsch, Positive quantum lyapunov exponents in experimental systems with a regular classical limit, *Phys. Rev. E* **101**, 010202 (2020).
- [25] T. Xu, T. Scaffidi, and X. Cao, Does scrambling equal chaos?, *Phys. Rev. Lett.* **124**, 140602 (2020), [arXiv:1912.11063 \[cond-mat.stat-mech\]](#).
- [26] K. Hashimoto, K.-B. Huh, K.-Y. Kim, and R. Watanabe, Exponential growth of out-of-time-order correlator without chaos: inverted harmonic oscillator, *JHEP* **11**, 068, [arXiv:2007.04746 \[hep-th\]](#).
- [27] N. Dowling, P. Kos, and K. Modi, Scrambling Is Necessary but Not Sufficient for Chaos, *Phys. Rev. Lett.* **131**, 180403 (2023), [arXiv:2304.07319 \[quant-ph\]](#).
- [28] Y. Liao, A. Vikram, and V. Galitski, Many-body level statistics of single-particle quantum chaos, *Phys. Rev. Lett.* **125**, 250601 (2020), [arXiv:2005.08991 \[cond-mat.stat-mech\]](#).
- [29] M. Winer, S.-K. Jian, and B. Swingle, An exponential ramp in the quadratic Sachdev-Ye-Kitaev model, *Phys. Rev. Lett.* **125**, 250602 (2020), [arXiv:2006.15152 \[cond-mat.stat-mech\]](#).
- [30] The latter model may be seen as bosonic counterparts for the SYK₂ model.
- [31] P. Hayden, M. Headrick, and A. Maloney, Holographic Mutual Information is Monogamous, *Phys. Rev. D* **87**, 046003 (2013), [arXiv:1107.2940 \[hep-th\]](#).
- [32] C. Weedbrook, S. Pirandola, R. García-Patrón, N. J. Cerf, T. C. Ralph, J. H. Shapiro, and S. Lloyd, Gaussian quantum information, *Rev. Mod. Phys.* **84**, 621 (2012).
- [33] H.-S. Zhong, H. Wang, Y.-H. Deng, M.-C. Chen, L.-C. Peng, Y.-H. Luo, J. Qin, D. Wu, X. Ding, Y. Hu, P. Hu, X.-Y. Yang, W.-J. Zhang, H. Li, Y. Li, X. Jiang, L. Gan, G. Yang, L. You, Z. Wang, L. Li, N.-L. Liu, C.-Y. Lu, and J.-W. Pan, Quantum computational advantage using photons, *Science* **370**, 1460 (2020), <https://www.science.org/doi/pdf/10.1126/science.abe8770>.
- [34] H.-S. Zhong, Y.-H. Deng, J. Qin, H. Wang, M.-C. Chen, L.-C. Peng, Y.-H. Luo, D. Wu, S.-Q. Gong, H. Su, Y. Hu, P. Hu, X.-Y. Yang, W.-J. Zhang, H. Li, Y. Li, X. Jiang, L. Gan, G. Yang, L. You, Z. Wang, L. Li, N.-L. Liu, J. J. Renema, C.-Y. Lu, and J.-W. Pan, Phase-programmable gaussian boson sampling using stimulated squeezed light, *Phys. Rev. Lett.* **127**, 180502 (2021).

- [35] L. S. Madsen, F. Laudenbach, M. F. Askarani, F. Rortais, T. Vincent, J. F. F. Bulmer, F. M. Miatto, L. Neuhaus, L. G. Helt, M. J. Collins, A. E. Lita, T. Gerrits, S. W. Nam, V. D. Vaidya, M. Menotti, I. Dhand, Z. Vernon, N. Quesada, and J. Lavoie, Quantum computational advantage with a programmable photonic processor, *Nature* **606**, 75 (2022).
- [36] Y.-H. Deng, Y.-C. Gu, H.-L. Liu, S.-Q. Gong, H. Su, Z.-J. Zhang, H.-Y. Tang, M.-H. Jia, J.-M. Xu, M.-C. Chen, J. Qin, L.-C. Peng, J. Yan, Y. Hu, J. Huang, H. Li, Y. Li, Y. Chen, X. Jiang, L. Gan, G. Yang, L. You, L. Li, H.-S. Zhong, H. Wang, N.-L. Liu, J. J. Renema, C.-Y. Lu, and J.-W. Pan, Gaussian boson sampling with pseudo-photon-number-resolving detectors and quantum computational advantage, *Phys. Rev. Lett.* **131**, 150601 (2023).
- [37] A. Serafini, *Quantum Continuous Variables: A Primer of Theoretical Methods* (CRC press, 2017).
- [38] In general, \mathbf{M} can be a Hermitian matrix, which can then be written as a sum of real symmetric and anti-symmetric matrices, $\mathbf{M} = \mathbf{M}_{\text{sym}} + i\mathbf{M}_{\text{asy}}$. However, the anti-symmetric part \mathbf{M}_{asy} only contributes an overall phase that can be ignored.
- [39] A holographic CFT is defined by a large number of degrees of freedom (large central charge in $2d$) and a sparse spectrum, i.e. a large gap between low spin and high spin operators.
- [40] A. Allais and E. Tonni, Holographic evolution of the mutual information, *JHEP* **01**, 102, arXiv:1110.1607 [hep-th].
- [41] V. Balasubramanian, A. Bernamonti, N. Copland, B. Craps, and F. Galli, Thermalization of mutual and tripartite information in strongly coupled two dimensional conformal field theories, *Phys. Rev. D* **84**, 105017 (2011), arXiv:1110.0488 [hep-th].
- [42] C. T. Asplund and A. Bernamonti, Mutual information after a local quench in conformal field theory, *Phys. Rev. D* **89**, 066015 (2014), arXiv:1311.4173 [hep-th].
- [43] S. Leichenauer and M. Moosa, Entanglement Tsunami in (1+1)-Dimensions, *Phys. Rev. D* **92**, 126004 (2015), arXiv:1505.04225 [hep-th].
- [44] L. Piroli, B. Bertini, J. I. Cirac, and T. c. v. Prosen, Exact dynamics in dual-unitary quantum circuits, *Phys. Rev. B* **101**, 094304 (2020).
- [45] A. Coser, E. Tonni, and P. Calabrese, Entanglement negativity after a global quantum quench, *J. Stat. Mech.* **1412**, P12017 (2014), arXiv:1410.0900 [cond-mat.stat-mech].
- [46] P. Calabrese and J. L. Cardy, Evolution of entanglement entropy in one-dimensional systems, *J. Stat. Mech.* **0504**, P04010 (2005), arXiv:cond-mat/0503393.
- [47] V. Alba and P. Calabrese, Entanglement and thermodynamics after a quantum quench in integrable systems, *Proc. Nat. Acad. Sci.* **114**, 7947 (2017).
- [48] V. Alba and P. Calabrese, Entanglement dynamics after quantum quenches in generic integrable systems, *SciPost Phys.* **4**, 017 (2018), arXiv:1712.07529 [cond-mat.stat-mech].
- [49] B. Bertini, P. Kos, and T. Prosen, Entanglement spreading in a minimal model of maximal many-body quantum chaos, *Phys. Rev. X* **9**, 021033 (2019), arXiv:1812.05090 [cond-mat.stat-mech].
- [50] L. Piroli, B. Bertini, J. I. Cirac, and T. Prosen, Exact dynamics in dual-unitary quantum circuits, *Phys. Rev. B* **101**, 094304 (2020), arXiv:1911.11175 [cond-mat.stat-mech].
- [51] A. Chan, A. De Luca, and J. T. Chalker, Solution of a minimal model for many-body quantum chaos, *Phys. Rev. X* **8**, 041019 (2018), arXiv:1712.06836 [cond-mat.stat-mech].
- [52] R. Modak, V. Alba, and P. Calabrese, Entanglement revivals as a probe of scrambling in finite quantum systems, *J. Stat. Mech.* **2008**, 083110 (2020), arXiv:2004.08706 [cond-mat.stat-mech].
- [53] K. Goto, A. Mollabashi, M. Nozaki, K. Tamaoka, and M. T. Tan, Information scrambling versus quantum revival through the lens of operator entanglement, *JHEP* **06**, 100, arXiv:2112.00802 [hep-th].
- [54] S. Rahimi-Keshari, S. Baghbanzadeh, and C. M. Caves, In situ characterization of linear-optical networks in randomized boson sampling, *Phys. Rev. A* **101**, 043809 (2020).
- [55] H. Casini and M. Huerta, Remarks on the entanglement entropy for disconnected regions, *JHEP* **03**, 048, arXiv:0812.1773 [hep-th].
- [56] M. Rangamani and M. Rota, Entanglement structures in qubit systems, *J. Phys. A* **48**, 385301 (2015), arXiv:1505.03696 [hep-th].
- [57] M. Rota, Tripartite information of highly entangled states, *JHEP* **04**, 075, arXiv:1512.03751 [hep-th].
- [58] C. A. Agón, P. Bueno, and H. Casini, Tripartite information at long distances, *SciPost Phys.* **12**, 153 (2022), arXiv:2109.09179 [hep-th].
- [59] A. Seshadri, V. Madhok, and A. Lakshminarayanan, Tripartite mutual information, entanglement, and scrambling in permutation symmetric systems with an application to quantum chaos, *Phys. Rev. E* **98**, 052205 (2018), arXiv:1806.00113 [quant-ph].
- [60] O. Schnaack, N. Bölter, S. Paeckel, S. R. Manmana, S. Kehrein, and M. Schmitt, Tripartite information, scrambling, and the role of Hilbert space partitioning in quantum lattice models, *Phys. Rev. B* **100**, 224302 (2019), arXiv:1808.05646 [cond-mat.str-el].
- [61] F. Caceffo and V. Alba, Negative tripartite mutual information after quantum quenches in integrable systems, *Phys. Rev. B* **108**, 134434 (2023).

- [62] G. Lo Monaco, L. Innocenti, D. Cilluffo, D. A. Chisholm, S. Lorenzo, and G. M. Palma, Quantum scrambling via accessible tripartite information, *Quantum Sci. Technol.* **8**, 035006 (2023), arXiv:2305.19334 [quant-ph].
- [63] S. Xu and B. Swingle, Scrambling dynamics and out-of-time-ordered correlators in quantum many-body systems, *PRX Quantum* **5**, 010201 (2024).
- [64] G. Adesso, D. Girolami, and A. Serafini, Measuring gaussian quantum information and correlations using the rényi entropy of order 2, *Phys. Rev. Lett.* **109**, 190502 (2012).
- [65] M. R. M. Mozaffar and A. Mollabashi, Time scaling of entanglement in integrable scale-invariant theories, *Phys. Rev. Res.* **4**, L022010 (2022), arXiv:2106.14700 [hep-th].
- [66] K. Hashimoto, K. Murata, and R. Yoshii, Out-of-time-order correlators in quantum mechanics, *JHEP* **10**, 138, arXiv:1703.09435 [hep-th].
- [67] R. J. Glauber, Photon correlations, *Phys. Rev. Lett.* **10**, 84 (1963).
- [68] E. C. G. Sudarshan, Equivalence of semiclassical and quantum mechanical descriptions of statistical light beams, *Phys. Rev. Lett.* **10**, 277 (1963).
- [69] K. E. Cahill and R. J. Glauber, Density operators and quasiprobability distributions, *Phys. Rev.* **177**, 1882 (1969).

Appendix A: Derivation of out-of-time-order correlators for quadrature operators

We derive Eq. (6), OTOC for canonical operators, and the ground state of quadratic Hamiltonians whose matrix \mathbf{M} can be diagonalized using symplectic transformations of the form $\mathbf{S} = \mathbf{S}_q \oplus \mathbf{S}_p$. This includes KG, DKG, and our random model (IIIb) Hamiltonians. We define

$$H_{\mathbb{D}} = U^\dagger H U = \frac{1}{2} U^\dagger r^\top U M U^\dagger r U = \frac{1}{2} r^\top \mathbf{D} r \quad (7)$$

where we used $U^\dagger r U = \mathbf{S} r$ and matrix $\mathbf{D} = \mathbf{S}^\top \mathbf{M} \mathbf{S}$ is diagonal.

Assuming that $\mathbf{S} = \mathbf{S}_q \oplus \mathbf{S}_p$, we have

$$\begin{aligned} \left[e^{iH_{\mathbb{D}}t} U^\dagger q_j U e^{-iH_{\mathbb{D}}t}, U^\dagger p_k U \right] &= \sum_{n,m} \mathbf{S}_{q,jn} \mathbf{S}_{p,km} \left[e^{iH_{\mathbb{D}}t} q_n e^{-iH_{\mathbb{D}}t}, p_m \right] \\ &= \sum_{n,m} \mathbf{S}_{q,jn} \mathbf{S}_{p,km} \left[q_n \cos(\omega_k t) + p_n \sin(\omega_k t), p_m \right] \\ &= i \sum_n \mathbf{S}_{q,jn} \mathbf{S}_{p,kn} \cos(\omega_n t) \\ &= i \left(\mathbf{S}_q \text{diag}(\cos(\omega_1 t), \dots, \cos(\omega_N t)) \mathbf{S}_p^\top \right)_{ij}, \end{aligned}$$

where we used $e^{iH_{\mathbb{D}}t} q_n e^{-iH_{\mathbb{D}}t} = q_n \cos(\omega_k t) + p_n \sin(\omega_k t)$ in the second line, and $[q_n, p_m] = i\delta_{nm}$ in the third line. Using the above relation and $H = U H_{\mathbb{D}} U^\dagger$, OTOC for canonical operators reads

$$\begin{aligned} C_{\beta,jk}(t) &= -\text{tr} \left(\frac{e^{-\beta H}}{\text{tr}(e^{-\beta H})} [q_j(t), p_k]^2 \right) \\ &= -\text{tr} \left(\frac{e^{-\beta H_{\mathbb{D}}}}{\text{tr}(e^{-\beta H_{\mathbb{D}}})} \left[e^{iH_{\mathbb{D}}t} U^\dagger q_j U e^{-iH_{\mathbb{D}}t}, U^\dagger p_j U \right]^2 \right) \\ &= \left(\mathbf{S}_q \text{diag}(\cos(\omega_1 t), \dots, \cos(\omega_N t)) \mathbf{S}_p^\top \right)_{ij}^2, \end{aligned} \quad (8)$$

which is Eq. (6) in the main text. This expression can be viewed as a generalization of the same quantity for a single oscillator previously reported in [66].

Appendix B: Out-of-time-order correlators for generic bosonic operators

Considering an N -mode bosonic system with the Hamiltonian H and local operators W_j and V_k acting on the j th and k th modes, respectively, OTOC can alternatively be defined as

$$F_{\beta,jk}(t) = \left\langle W_j^\dagger(t) V_k^\dagger W_j(t) V_k \right\rangle = \text{tr} \left(\frac{e^{-\beta H}}{\text{tr}(e^{-\beta H})} W_j^\dagger(t) V_k^\dagger W_j(t) V_k \right), \quad (9)$$

where $W_j(t) = e^{-itH} W_j e^{itH}$. Note that if W_j and V_k are unitary, then the relation between this quantity and $C_{\beta,jk}(t) = \langle [V_k, W_j(t)]^\dagger [V_k, W_j(t)] \rangle$, which is used in the main text, is given by $\text{Re}[F_{\beta,jk}(t)] = 1 - C_{\beta,jk}(t)/2$. Here, we consider passive Hamiltonians that can be transformed into an uncoupled Hamiltonian of harmonic oscillators using a passive Gaussian unitary,

$$H = (a_1, \dots, a_N) \mathbf{M} (a_1^\dagger, \dots, a_N^\dagger)^\top = U_p H_D U_p^\dagger \quad (10)$$

with $H_D = \sum_j \omega_j a_j^\dagger a_j$. The passive unitary can be described by $U_p^\dagger a_j^\dagger U_p = \sum_n \mathbf{U}_{jn} a_n^\dagger$ with \mathbf{U}_{jn} being the elements of the $N \times N$ unitary matrix that diagonalizes the Hamiltonian matrix, $\sum_{jk} \mathbf{U}_{mk}^* \mathbf{M}_{kj} \mathbf{U}_{jn} = \omega_n \delta_{nm}$. By using this transformation, we have

$$F_{\beta,jk}(t) = \text{tr} \left(\frac{e^{-\beta H_D}}{\text{tr}(e^{-\beta H_D})} \tilde{W}_j^\dagger(t) \tilde{V}_k^\dagger \tilde{W}_j(t) \tilde{V}_k \right) \quad (11)$$

where $\tilde{W}_j(t) = e^{itH_D} U_p^\dagger W_j U_p e^{-itH_D}$ and $\tilde{V}_k = U_p^\dagger V_k U_p$.

The thermal state of N -mode uncoupled system can be expressed in terms of multimode coherent states $|\alpha_1, \dots, \alpha_N\rangle$ using the Glauber-Sudarshan representation [67, 68]

$$\frac{e^{-\beta H_D}}{\text{tr}(e^{-\beta H_D})} = \int \cdots \int d^2\alpha_1 \cdots d^2\alpha_N \frac{e^{-|\alpha_1|^2/\bar{n}_1}}{\bar{n}_1\pi} \times \cdots \times \frac{e^{-|\alpha_N|^2/\bar{n}_N}}{\bar{n}_N\pi} |\alpha_1, \dots, \alpha_N\rangle \langle \alpha_1, \dots, \alpha_N| \quad (12)$$

with $\bar{n}_j = (e^{\beta\omega_j} - 1)^{-1}$ being the mean photon number in the j th mode. Using this, we can write

$$F_{\beta,jk}(t) = \int d^{2N}\boldsymbol{\alpha} P(\boldsymbol{\alpha}) \tilde{F}_{\boldsymbol{\alpha},jk}(t), \quad (13)$$

where $\boldsymbol{\alpha} = (\alpha_1, \dots, \alpha_N)$, $P(\boldsymbol{\alpha}) = \prod_{j=1}^N \exp(-|\alpha_j|^2/\bar{n}_j)/(\bar{n}_j\pi)$, and

$$\tilde{F}_{\boldsymbol{\alpha},jk}(t) = \langle \alpha_1, \dots, \alpha_N | \tilde{W}_j^\dagger(t) \tilde{V}_k^\dagger \tilde{W}_j(t) \tilde{V}_k | \alpha_1, \dots, \alpha_N \rangle \quad (14)$$

is the OTOC in terms of coherent states. Note that for $\beta = \infty$ (zero temperature) $F_{\infty,jk}(t) = \tilde{F}_{\mathbf{0},jk}(t)$.

The operators can also be expanded in terms of displacement operators $D_j(\zeta) = \exp(\zeta a_j^\dagger - \zeta^* a_j)$ with $\zeta \in \mathbb{C}$ [69]

$$W_j = \frac{1}{\pi} \int d^2\zeta \Phi_{W_j}(\zeta) D_j(-\zeta), \quad (15)$$

where $\Phi_{W_j}(\zeta) = \text{tr}(W_j D_j(\zeta))$ is the characteristic function of operator W_j . We have

$$U_p^\dagger D_j(\zeta) U_p = D_1(\zeta \mathbf{U}_{j1}) \otimes \cdots \otimes D_N(\zeta \mathbf{U}_{jN}), \quad (16)$$

where we used $U_p^\dagger a_j^\dagger U_p = \sum_n \mathbf{U}_{jn} a_n^\dagger$, and also

$$e^{itH_D} D_j(\zeta) e^{-itH_D} = D_j(\zeta e^{it\omega_j}). \quad (17)$$

Using these two relations we can then compute

$$\tilde{W}_j(t) = e^{itH_D} U_p^\dagger W_j U_p e^{-itH_D} = \frac{1}{\pi} \int d^2\zeta \Phi_{W_j}(\zeta) D_1(-\zeta \mathbf{U}_{j1} e^{it\omega_1}) \otimes \cdots \otimes D_N(-\zeta \mathbf{U}_{jN} e^{it\omega_N}). \quad (18)$$

Therefore, by using a similar expression for \tilde{V}_k , the OTOC in terms of coherent states can be written as

$$\begin{aligned} \tilde{F}_{\alpha,jk}(t) &= \frac{1}{\pi^4} \int d^2\zeta d^2\xi d^2\beta d^2\gamma \Phi_{W_j}^*(\zeta) \Phi_{V_k}^*(\xi) \Phi_{W_j}(\beta) \Phi_{V_k}(\gamma) \\ &\times \prod_{n=1}^N \langle \alpha_n | D_n(\zeta \mathbf{U}_{jn} e^{it\omega_n}) D_n(\xi \mathbf{U}_{kn}) D_n(-\beta \mathbf{U}_{jn} e^{it\omega_n}) D_n(-\gamma \mathbf{U}_{kn}) | \alpha_n \rangle. \end{aligned} \quad (19)$$

As we can see each term in the product oscillates with time with frequency ω_n . By using the following relation for displacement operators

$$D_n(\mu) D_n(\nu) = \exp\left(\frac{\mu\nu^* - \nu\mu^*}{2}\right) D_n(\mu + \nu), \quad (20)$$

we get

$$\begin{aligned} D_n(\zeta \mathbf{U}_{jn} e^{it\omega_n}) D_n(\xi \mathbf{U}_{kn}) D_n(-\beta \mathbf{U}_{jn} e^{it\omega_n}) D_n(-\gamma \mathbf{U}_{kn}) &= D_n(\mathbf{U}_{jn} e^{it\omega_n} (\zeta - \beta) + \mathbf{U}_{kn} (\xi - \gamma)) \\ &\times \exp\left[\frac{1}{2} \left((\zeta\xi^* + \beta\gamma^* + \beta\xi^* - \zeta\gamma^*) \mathbf{U}_{jn} e^{i\omega_n t} \mathbf{U}_{kn}^* + \gamma\xi^* |\mathbf{U}_{kn}|^2 + \beta\zeta^* |\mathbf{U}_{jn}|^2 \right) - \text{c.c.} \right], \end{aligned} \quad (21)$$

where c.c. stands for complex conjugate. We also have $\langle \alpha | D(\mu) | \alpha \rangle = \exp(-|\mu|^2/2 + \mu\alpha^* - \alpha\mu^*)$. Using these equations, Eq. (19) becomes

$$\begin{aligned} \tilde{F}_{\alpha,jk}(t) &= \frac{1}{\pi^4} \int d^2\zeta d^2\xi d^2\beta d^2\gamma \Phi_{W_j}^*(\zeta) \Phi_{V_k}^*(\xi) \Phi_{W_j}(\beta) \Phi_{V_k}(\gamma) \\ &\times \exp\left[-\frac{1}{2} |\zeta - \beta|^2 - \frac{1}{2} |\xi - \gamma|^2 - \frac{1}{2} ((\zeta - \beta)(\xi^* - \gamma^*) \mathbf{V}_{jk}(t) + \text{c.c.})\right] \\ &\times \exp\left[\left((\zeta - \beta) \sum_{n=1}^N \mathbf{U}_{jn} e^{it\omega_n} \alpha_n^* + (\xi - \gamma) \sum_{n=1}^N \mathbf{U}_{kn} \alpha_n^*\right) - \text{c.c.}\right] \\ &\times \exp\left[\frac{1}{2} \left((\zeta\xi^* + \beta\gamma^* + \beta\xi^* - \zeta\gamma^*) \mathbf{V}_{jk}(t) + \gamma\xi^* + \beta\zeta^* \right) - \text{c.c.}\right], \end{aligned} \quad (22)$$

where we used $\sum_n |\mathbf{U}_{jn}|^2 = 1$ and

$$\mathbf{V}_{jk}(t) = \sum_{n=1}^N \mathbf{U}_{jn} e^{i\omega_n t} \mathbf{U}_{kn}^* \quad (23)$$

is an element of the unitary matrix $\mathbf{V}(t) = \exp(i\mathbf{M}t)$, where \mathbf{M} is the Hamiltonian matrix in Eq. (10). Given the characteristic functions Φ_{V_k} and Φ_{W_j} , one can therefore compute $F_{\alpha,jk}(t)$ and then by averaging with respect to $P(\alpha)$ in Eq. (13), $F_{\beta,jk}(t)$ can be obtained.

As a simple example, suppose that $W_j = D_j(\mu)$ and $V_k = D_k(\nu)$ are displacement operators with the characteristic functions $\Phi_{W_j}(\beta) = \pi\delta^2(\beta + \mu)$ and $\Phi_{V_k}(\gamma) = \pi\delta^2(\gamma + \nu)$. In this case, we have

$$\tilde{F}_{\alpha,jk}(t) = \exp(\mu\nu^* \mathbf{V}_{jk}(t) - \mu^* \nu \mathbf{V}_{jk}^*(t)), \quad (24)$$

which implies that $F_{\beta,jk}(t) = \tilde{F}_{\alpha,jk}(t)$ is independent of β . This also gives $C_{\beta,jk}(t) = 2 - 2\text{Re}[F_{\beta,jk}(t)] = 4\sin^2(\text{Im}[\mu\nu^* \mathbf{V}_{jk}(t)])$.

In this example, we can see that the time-dependent behavior of OTOC is determined by that of $\mathbf{V}_{jk}(t)$. Therefore, to further investigate the time-dependent behaviour of $\mathbf{V}_{jk}(t)$, we ran numerical simulations for a randomly selected set of $\{\omega_n\}$ and \mathbf{U} selected as a $N \times N$ unitary matrix chosen from the Haar measure. As shown in the left panel of Fig. 5, $\mathbf{V}_{jk}(t)$ rapidly saturates to a constant value at some time $t_* \sim 1/\log N$. The larger the system size, the faster $\mathbf{V}_{jk}(t)$ and the OTOC saturation. Note that this behavior is critically different from the scrambling time $t_s \sim \log N$ in generic chaotic systems. Due to this rapid saturation, OTOC does not have enough time to oscillate except for the

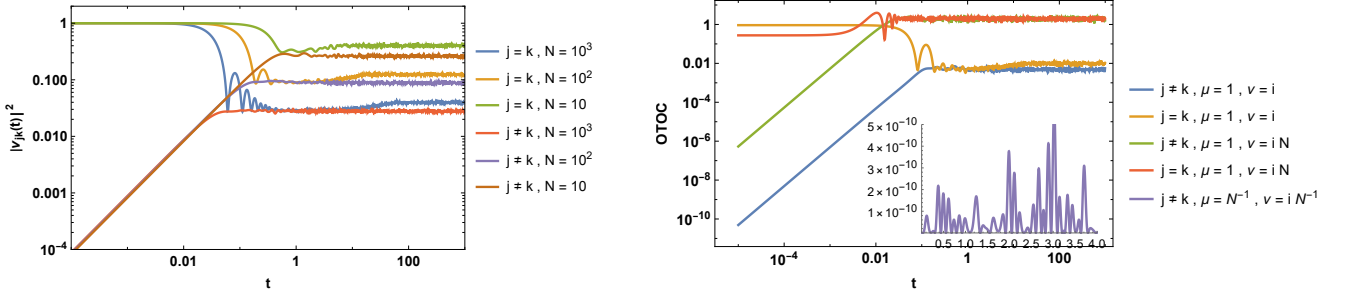


FIG. 5. Right: Time evolution of the diagonal and off-diagonal elements of $\mathbf{V}_{jk}(t)$. \mathbf{U} is a Haar random unitary matrix and the result is averaged over 200 samples. Left: The behavior of OTOC $F_{\beta,jk}(t)$ for displacement operators with parameters μ and ν . The inset shows the choice of $\mu\nu^* \sim 1/N^2$ is small enough to compensate for the rapid saturation of $\mathbf{V}_{jk}(t)$ and allow the OTOC to oscillate in time.

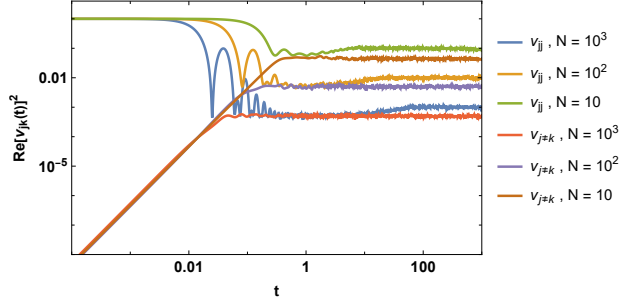


FIG. 6. The behavior of OTOC $C_{\infty,jk}(t)$ for the canonical operators $V = q_j$ and $W = p_k$. The results are averaged over 300 samples.

cases where the parameters in $W_j = D_j(\mu)$ and $V_k = D_k(\nu)$ slow down this rapid saturation time (see the inset of the right panel in Fig. 5).

Another example is to consider canonical operators as local operators $W_j = q_j = (a_j + a_j^\dagger)/\sqrt{2}$ and $V_k = p_k = -i(a_k - a_k^\dagger)/\sqrt{2}$ whose characteristic functions are $\Phi_{W_j}(\beta) = \pi(\frac{\partial}{\partial\beta} - \frac{\partial}{\partial\beta^*})\delta^2(\beta)/\sqrt{2}$ and $\Phi_{V_k}(\gamma) = i\pi(\frac{\partial}{\partial\gamma} + \frac{\partial}{\partial\gamma^*})\delta^2(\gamma)/\sqrt{2}$. Plugging these into (22) for $\alpha = \mathbf{0}$ and using integration by parts yields

$$\tilde{F}_{\mathbf{0},jk}(t) = F_{\infty,jk}(t) = \frac{1}{4} \left(1 + |\mathbf{V}_{jk}(t)|^2 - \mathbf{V}_{jk}^{*2}(t) \right) \quad (25)$$

which is again governed by the behaviour of $\mathbf{V}_{jk}(t)$. Using the above formalism, it is straightforward to show that the other definition of OTOC at zero temperature is given by

$$C_{\infty,jk}(t) = \frac{1}{4} \left(2|\mathbf{V}_{jk}(t)|^2 + \mathbf{V}_{jk}^2(t) + \mathbf{V}_{jk}^{*2}(t) \right) = [\text{Re}(\mathbf{V}_{jk}(t))]^2. \quad (26)$$

As shown in Fig. 6, this function shows a power law growth, similar to the behavior in Fig. 5. Note that for a single oscillator, this is a periodic function (see Eq. (6) and [66]) while for $N > 1$ the role of $\mathbf{V}_{jk}(t)$ becomes important.

The above formalism can also be applied to compute OTOC for $q_j^{n_q}$ and $p_k^{n_p}$. In this case, the characteristic functions are given in terms of higher-order partial derivatives of the Dirac delta function (22) that results in an integer power of $\text{Im}(\mathbf{V}_{jk}(t))$ and $\text{Re}(\mathbf{V}_{jk}(t))$ in OTOC. Note that, in general, due to the rapid saturation of $\mathbf{V}_{jk}(t)$, the result of OTOC reduces to a power law in t .

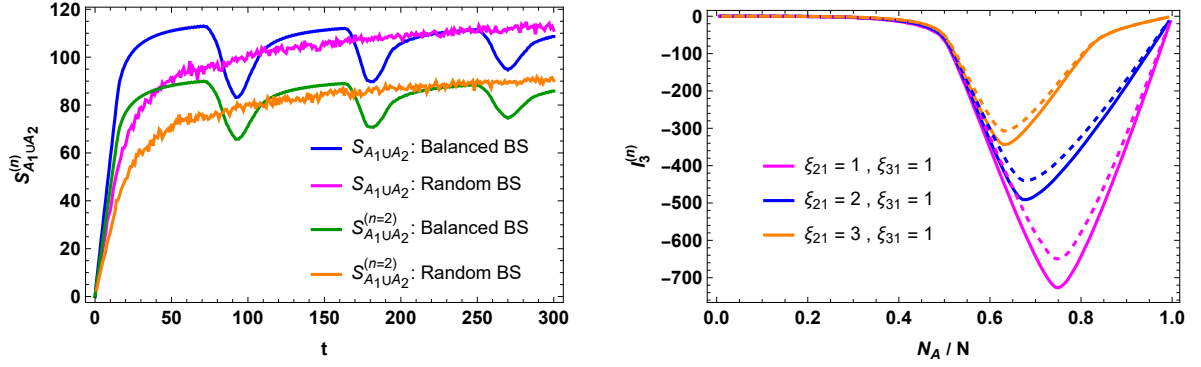


FIG. 7. Left: Entanglement in the passive circuit model (IIb) for disjoint blocks compared with Rényi-2. The initial state is the tensor product of single-mode squeezed vacuum states with $\lambda_i = 2$. We set $N_{A_1} = N_{A_2} = 40$ and $d = 200$. We consider the beam splitter (BS) transfer matrix \mathbf{U}_{BS} chosen randomly at every single time step. For a balanced BS, we observe memory effects for both the entanglement and the Rényi-2 case. The second and third dips in the blue and green curves correspond to entanglement revivals. All random results are averaged over 300 samples. Right: I_3 for random model (IIa), where the tensor product of squeezed-vacuum states ($\lambda_i = 5$) is evolved by a one-step N -mode passive network described by a Haar random unitary. We set $N = 500$ and $\xi_{ij} \equiv \frac{N_{A_i}}{N_{A_j}}$. The dashed curves correspond to the Rényi-2 version of TMI with the same parameters as the solid curves.

Appendix C: Information scrambling in terms of the Rényi-2 entropy

We observe that replacing the von Neuman entropy by Rényi-2 entropy leads to similar results for information scrambling in Gaussian states. The Rényi-2 entropy for Gaussian states takes a simple form in terms of the determinant of the covariance matrix of the state [64]

$$S^{(2)}(\rho) = -\ln \text{tr}(\rho^2) = \frac{1}{2} \ln \det(\boldsymbol{\sigma}). \quad (27)$$

As shown in Fig. 7, the dynamics of the entanglement and the TMI in terms of the Rényi-2 entropy have similar behavior to the corresponding quantities in terms of the von Neumann entropy, presented in the main text.

As discussed, the Wigner function of Gaussian states is a normalized Gaussian function

$$W_\rho(\boldsymbol{\alpha}) = \frac{1}{\pi^N \sqrt{\det(\boldsymbol{\sigma})}} e^{-\boldsymbol{\alpha}^\top \boldsymbol{\sigma}^{-1} \boldsymbol{\alpha}}, \quad (28)$$

where $\boldsymbol{\alpha} \in \mathbb{R}^{2N}$. Hence, the Gaussian Wigner function can be viewed as a probability density, and its continuous Shannon entropy up to an additional constant is equal to the Rényi-2 entropy of the state [64],

$$H(W_\rho) = -\int d^{2N} \boldsymbol{\alpha} W_\rho(\boldsymbol{\alpha}) \ln(W_\rho(\boldsymbol{\alpha})) = S^{(2)}(\rho) + N(1 + \ln \pi). \quad (29)$$

This is in fact the entropy of the classical random variable $\boldsymbol{\alpha}$ sampled from the Wigner function.

This relation between the continuous Shannon entropy and the Rényi-2 entropy implies that information scrambling in our quantum setup can analogously be observed in a classical setup involving Gaussian random variables. Specifically, one can generate Gaussian random variables according to the Wigner function of the initial state, which are then evolved according to the Gaussian dynamics. Given Eq. (29) and the results presented in Fig. 7, it can be seen that similar information scrambling features can be observed in terms of the entropy of the Gaussian random variables in analogous classical setups.